AFGL-TR-87-0225
ENVIRONMENTAL RESEARCH PAPERS, NO. 980

AD-A196 228

Particle Trajectories and Potentials in a Plane Sheath Moving in a Magnetoplasma

CHARLES W. DUBS
DAVID L. COOKE

15 July 1987

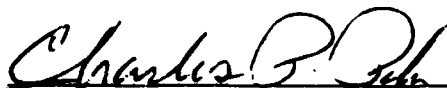SPACE PHYSICS DIVISION   PROJECT 7601
AIR FORCE GEOPHYSICS LABORATORY
HANSCOM AFB, MA 01731

AFGL-TR-87-0225
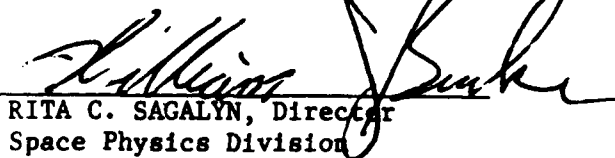
"This technical report has been reviewed and is approved for publication"

FOR THE COMMANDER

CHARLES P. PIKE, Chief
Spacecraft Interactions Branch
Space Physics Division

RITA C. SAGALYN, Director
Space Physics Division

REPORT DOCUMENTATION PAGE		Form Approved OMB No. 0704-0188

1a. REPORT SECURITY CLASSIFICATION Unclassified	1b. RESTRICTIVE MARKINGS
2a. SECURITY CLASSIFICATION AUTHORITY	3. DISTRIBUTION/AVAILABILITY OF REPORT
2b. DECLASSIFICATION/DOWNGRADING SCHEDULE	Approved for public release; distribution unlimited.

4. PERFORMING ORGANIZATION REPORT NUMBER(S) AFGL-TR-87-0225 ERP, No. 980	5. MONITORING ORGANIZATION REPORT NUMBER(S)

6a. NAME OF PERFORMING ORGANIZATION Air Force Geophysics Laboratory	6b. OFFICE SYMBOL (If applicable) PHK	7a. NAME OF MONITORING ORGANIZATION Air Force Geophysics Laboratory

6c. ADDRESS (City, State, and ZIP Code) Hanscom AFB Massachusetts 01731	7b. ADDRESS (City, State, and ZIP Code) Hanscom AFB Massachusetts 01731

8a. NAME OF FUNDING/SPONSORING ORGANIZATION	8b. OFFICE SYMBOL (If applicable)	9. PROCUREMENT INSTRUMENT IDENTIFICATION NUMBER

8c. ADDRESS (City, State, and ZIP Code)	10. SOURCE OF FUNDING NUMBERS			
	PROGRAM ELEMENT NO.	PROJECT NO.	TASK NO	WORK UNIT ACCESSION NO
	62101F	76-01	30	01

11. TITLE (Include Security Classification)
Particle Trajectories and Potentials in a Plane Sheath Moving in a Magnetoplasma

12. PERSONAL AUTHOR(S) Charles W. Dubs and David L. Cooke

13a. TYPE OF REPORT Scientific. Interim.	13b. TIME COVERED FROM _____ TO _____	14. DATE OF REPORT (Year, Month, Day) 1987 July 15	15 PAGE COUNT 34

16. SUPPLEMENTARY NOTATION

17. COSATI CODES			18. SUBJECT TERMS (Continue on reverse if necessary and identify by block number)
FIELD	GROUP	SUB-GROUP	Plane sheath, Magnetic field
			Analytical solution, Electric field
			Moving plasma, Particle trajectory

19. ABSTRACT (Continue on reverse if necessary and identify by block number)

A plane sheath moving in the direction of its normal across the magnetic field through a magnetoplasma is analyzed. The self consistent analytic solution for electric field and trajectories of univelocity attracted particles as a function of sheath edge entry angle is derived. For simplicity, the sheath edge is assumed to be sharp. The solution is similar to that for a planar magnetron found much earlier. A quantity q, the square of the ratio of plasma frequency to gyrofrequency, is found to be critical in the behavior of the attracted species. If it is more than a limiting (cutoff) value, q_m, that depends only on entry angle and Mach number, M, the particles penetrate the whole sheath; if it is less than q_m, there is a turning point. If this point is in the sheath, some or all of the particles return to the sheath edge. In the frame of the object plane, for $M \ll 1$, q_m is $1/(2M)$ at vertical and ∞ at grazing incidence; for $M = 1$, $q_m = 1$; for $M \gg 1$, q_m is $1/2$. So the effect of magnetic field can increase greatly for drift velocity much less than thermal speed. The range of entry angles is derived. For typical low earth orbit -

20. DISTRIBUTION/AVAILABILITY OF ABSTRACT ☐ UNCLASSIFIED/UNLIMITED ☐ SAME AS RPT. ☐ DTIC USERS	21. ABSTRACT SECURITY CLASSIFICATION Unclassified
22a. NAME OF RESPONSIBLE INDIVIDUAL Charles W. Dubs	22b. TELEPHONE (Include Area Code) (617) 377-2932	22c OFFICE SYMBOL AFGL/PHK

18. (Contd)

Mach number   Insulation gap
Sheath entrance angle   Stability
Particle reflection

---

19. (Contd)

,conditions, electrons enter between grazing incidence and $45°$, and have a value of q less than a third of q_m, whereas 0^+ ions enter within $7°$ of vertical incidence and have a value of q over 10^5 times larger than q_m. So the magnetic field affects the electrons greatly but the ions only very slightly. For $q < q_m/2$ and sufficient object potential, the theory results in an insulation gap (no particles) next to the object surface. This gap increases with surface potential, even though stability analysis shows a tendency for the gap to vanish. However, taking reentry of attracted species and a velocity distribution into account indicates continuous penetration of some high energy particles to the object and, either conduction and insulation alternating periodically, or continuous conduction and reflection. Although the assumptions of a sharp sheath edge and only the attracted species entering the sheath at one velocity are limiting, the physical trends of the results should be correct.

Contents

Illustrations

Table

Particle Trajectories and Potentials in a Plane Sheath Moving in a Magnetoplasma

1. INTRODUCTION

In general, an analytic self consistent solution cannot be obtained for the interaction of a charged body with a magnetoplasma. The only exception found, the case treated here, is that of an infinite planar sheath parallel to the magnetic field. (For an infinite cylindrical magnetron, Page and Adams[1,2] obtained the cutoff radius, magnetic field, and a good approximation to the trajectories and electric field.) The solution for a crossed-field gap (plane diode, planar magnetron) is old (Benham,[3] Birdsall and Bridges[4] and references therein). Instead of emission from one plate toward a parallel plate, here only one plate (object plane) moving relative to a plasma is considered. Nevertheless, for the model considered, the cases are close enough for the solutions to be basically the same. For simplicity, we assume the sheath edge to be sharp and parallel to the object plane, collisions to be negligible,

1. Page, L., and Adams, N.I. (1946) Space charge in cylindrical magnetron, Phys. Rev., 69:494-500

2. Page, L., and Adams, N.I. (1958) Principles of Electricity, 3rd Ed., D. Van Nostrand.

3. Benham, W.E. (1935) Electronic theory and the magnetron oscillator Proc. Phys. Soc., (London) 47:1-53.

4. Birdsall, C.K., and Bridges, W.B. (1966) Electron Dynamics of Diode Regions, Academic Press, Chapter 5.

1

and all of the attracted particles to have the same sheath entry angle and perpen-
dicular component of energy. Whether or not the sheath edge may be considered
sharp depends on the relative values of various scale lengths such as Debye length,
repelled species ambient gyroradius, and total sheath thickness. By these criteria,
for the ionospheric applications envisioned, the sheath edge is not sharp. Even as
a poor approximation, however, the physical trends of the results obtained here
are expected to be correct. Without motion between the plasma and object, and the
collision mean free path much larger than the gyroradius as in the F layer of the
ionosphere, the steady state current density to such a surface would be negligible.
This is due to lack of a mechanism for charged particles continually to come
within two gyroradii of the sheath edge where their gyration could cause impact.
(A finite plane would actually receive appreciable current along the magnetic field
lines to and near the edge of the plane.) With motion, the solution is slightly
different from that for a planar magnetron. Here, cutoff or the amount of current
turned back is related to a function of parameters called q as defined and used by
Linson,[5] for example. The range of incidence angles for a moving object is calcu-
lated, the stability of a cutoff sheath is examined, and conclusions are drawn.

5. Linson, R. H. (1969) Current-voltage characteristics of an electron-emitting
   satellite in the ionosphere, J. Geophys. Res., 74:2368-2375.

2. TRAJECTORIES AND FIELDS

Figure 1 shows the coordinate system chosen. The sheath edge is at y_o, y_o^*, is perpendicular to y, y*, and is assumed to be sharp: the plasma is assumed neutral with no electric field for $y \leqq y_o$, and the repelled species is assumed not to penetrate to $y > y_o$. E_o, the electric field at $y = y_o$, is carried through the analysis anyway for generality and for the stability treatment. v_g is the component perpendicular to $\vec{B}$ of attracted species thermal velocity in the plasma frame. The plasma moves toward the object with a relative velocity v_d along y. $\vec{v}_o = \vec{v}_g + \vec{v}_d$. The attracted species is assumed to enter the sheath at an angle α^* in the plasma frame and α in the object frame. Calculation is made in the object frame. Figures 2 and 3 show qualitatively examples of trajectories; near the sheath edge for $\vec{B} = \hat{z}B$ and $B > 0$, positive particles move in the counterclockwise and negative in the clockwise sense. A dot over a quantity means its time derivative. The electric field is in the y direction, and the cylindrical radius, $\vec{R}$, is perpendicular to $\vec{B}$. So,
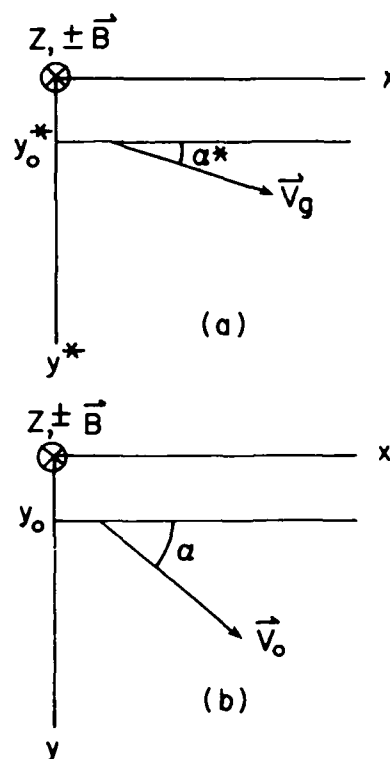

Figure 1. Coordinate System
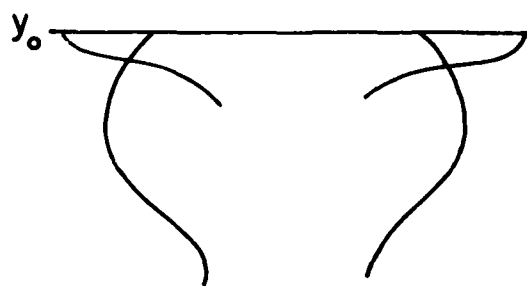(a) Plasma Frame and (b) Object Frame

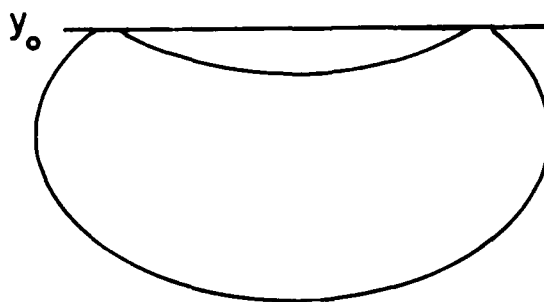Figure 2. Penetrating Trajectories

Figure 3. Reflecting Trajectories

$$\vec{R} \equiv \hat{x}x + \hat{y}y, \quad \vec{B} = p\hat{z}B, \quad p = \pm 1, \quad B > 0, \quad \vec{E} = \hat{y}E = -\hat{y}\,d\varphi/dy \;.$$

The initial, thermal, drift velocities, and entrance angle are related as follows:

$$\dot{x}_o = v_o \cos\alpha = v_g \cos\alpha^*, \quad \dot{y}_o = v_o \sin\alpha = v_g \sin\alpha^* + v_d,$$

$$v_o^2 = \dot{x}_o^2 + \dot{y}_o^2, \quad v_g^2 = \dot{x}_o^2 + (\dot{y}_o - v_d)^2 = v_o^2 - 2v_o v_d \sin\alpha + v_d^2 \;.$$

The differential equations for the attracted particles are the motion, energy, and Poisson equations:

$$\ddot{\vec{R}} = s\frac{e}{m}[\vec{E} + \dot{\vec{R}} \times \vec{B}]$$

$$\dot{R}^2 + s\frac{2e}{m}\varphi = v_o^2 + s\frac{2e}{m}\varphi_o = \text{const.}$$

$$-\frac{d^2\varphi}{dy^2} = s\frac{ne}{\epsilon_o} \;,$$

where $s = +1$ and -1 for the attracted species being ions (assumed positive, singly ionized) and electrons respectively, e is the magnitude of the electronic charge, and m is the mass of the attracted species. Except for ϵ_o, the subscript o denotes the initial value, the value at the sheath edge. The time t is chosen zero when the particle enters the sheath edge. Let

$$\omega \equiv eB/m, \quad \theta \equiv \omega t, \quad v_g \equiv \omega r_g, \quad X \equiv x/r_g, \quad Y \equiv y/r_g \;.$$

$$X' \equiv \frac{dX}{d\theta} = \dot{x}/v_g, \quad Y' \equiv \frac{dY}{d\theta} = \dot{y}/v_g, \quad \Phi \equiv s\frac{2e\varphi}{mv_g^2}, \quad -\frac{d\Phi}{dY} = \bar{E} \equiv s\frac{2e}{m\omega v_g}E \;,$$

$$q \equiv \frac{\omega_p^2}{\omega^2} = \frac{n_\infty m}{\epsilon_o B^2} = \frac{1}{2}\left[\frac{r_g}{\lambda_D}\right]^2, \quad M \equiv v_d/v_g \;,$$

$$V_o \equiv v_o/v_g = \sqrt{X_o'^2 + Y_o'^2} = \sqrt{1 + 2M\sin\alpha^* + M^2} \;,$$

$$X_o' = \cos\alpha^* = V_o\cos\alpha, \quad Y_o' = \sin\alpha^* + M = V_o\sin\alpha \;.$$

Differentiation by θ is denoted by a prime; n_∞ denotes the ambient plasma number density; M is the Mach number; λ_D is the Debye length. Normalizing thus, the differential equations become

$$X'' = sp Y' \tag{1'}$$

$$Y'' = \frac{1}{2}\overline{E} - sp X' \tag{2'}$$

$$X'^2 + Y'^2 + \Phi - 1 + 2M \sin \alpha^* + M^2 + \Phi_o \tag{3}$$

$$-\frac{d^2\Phi}{dY^2} = 2q\frac{n}{n_\infty} \ . \tag{4}$$

To treat both species simultaneously, we shall take p = s. Then Eqs. (1') and (2') become

$$X'' = Y' \tag{1}$$

$$Y'' = \frac{1}{2}\overline{E} - X' \ . \tag{2}$$

$q > 0$, $\Phi - \Phi_o \lesseqgtr 0$, and $\overline{E} \geqq 0$. Thus attracted electrons have the same normalized trajectory as attracted ions if $\vec{B}$ has (and φ and E have) the opposite sign.

Integrating Eq. (1),

$$X' = \cos \alpha^* + Y - Y_o \ . \tag{5}$$

Continuity of current provides the additional expression needed to determine the density. This expression, two of the first three equations, and Eq. (4) then constitute a close set. First, we consider three possible cases concerning trajectories. (See Section 3.)

(A) q is sufficiently large; $Y(\theta)$ increases and never decreases with θ, as in Figure 2. All of the current is transmitted and is assumed to be collected.

(B) Between the two limiting values of q, a fraction of the particles return and the rest are transmitted.

(C) q is sufficiently small, and object $|\Phi|$ and thus sheath edge to object distance, are sufficiently large; the particles all return as in Figure 3. This is the cutoff case with no net current.

How do the return and forward velocities compare? Since $\Phi = \Phi(Y)$ and, from Eq. (5), $X' = X'(Y)$, then from Eq. (3), for the same value of Y, $Y'_- = -Y'_+$, where $Y'_+ > 0$ and $Y'_- < 0$. So, the return part of a trajectory is symmetric to the $Y' > 0$ part.

Since the y component of incident particle flux equals the sweepout rate and the steady state current is conserved,

$$n_+ Y'_+ v_g = n_{0+} Y'_{0+} v_g = n_\infty v_d , \tag{6}$$

where n_+ and n_- denote the number density of particles having $Y' > 0$ and $Y' < 0$ respectively. This assumes that any returning particles exiting the sheath edge do not reenter the sheath. Then $n_{0+} = M n_\infty / Y'_0$. This $Y' > 0$ part of the current density is constant up to a turning point, $\theta (Y' = 0) = \tau$, if a turning point exists. Let $F - 1$ be the fraction of the incident current density that is returned if the collector is beyond a turning point. Then the return particle current density at the same value of Y is

$$-n_- Y'_- v_g = n_- Y'_+ v_g = (F - 1) n_\infty v_d . \tag{7}$$

Since steady state is assumed and no charge sources or sinks exist in the sheath, the net y component of flux is the same throughout the sheath. This then is $[1 - (F - 1)] n_\infty v_d$. $F = 1$ for Case A, $1 < F < 2$ for case B, and 2 for case C. Eq. (7) times n_+ divided by Eq. (6) shows that, for the same value of Y,

$$n_- = (F - 1) n_+ . \tag{8}$$

Before reaching any turning point,

$$n = n_- + n_+ = F M n_\infty / Y'_+ , \tag{9}$$

from the sum of Eqs. (6) and (7) divided by $Y'_+ v_g$. So, for all three cases, for $Y' > 0$, Eq. (4) becomes

$$-\frac{d^2 \Phi}{dY^2} = \frac{2 F M q}{Y'} . \tag{10}$$

Multiplying by $dY = Y' d\theta$ and integrating:

$$- d\Phi/dY = \overline{E} = \overline{E}_O + 2FMq\vartheta \quad . \tag{11}$$

From Eqs. (2), (5), and (11),

$$Y'' = FMq\theta + a + Y_O - Y , \tag{12}$$

where

$$a \equiv \overline{E}_O/2 - \cos \alpha^* . \tag{13}$$

This quantity has two parts: that due to the non-space-charge-limited initial electric field, and that due to the angle of the particle's incident velocity with the sheath normal.

The Ansatz $Y = -A \cos(\theta + \beta) + C\theta + D$ is substituted into Eq. (12). This and the initial conditions lead to the solution for $Y' \geq 0$.

$$Y = Y_O + a - A \cos(\theta + \beta) + FMq\theta \tag{14}$$

$$Y' = A \sin(\theta + \beta) + FMq \tag{15}$$

$$Y'' = A \cos(\theta + \beta) \tag{16}$$

$$A = \sqrt{a^2 + (Y_O' - FMq)^2} \tag{17}$$

$$\cos \beta = a/A = \frac{a}{|a|} \left[1 + \left(\frac{\sin \alpha^* + M - FMq}{\overline{E}_O/2 - \cos \alpha^*} \right)^2 \right]^{-1/2} \tag{18}$$

$$\sin \beta = (Y_O' - FMq)/A . \tag{19}$$

The quantity a is seen to be the Y component of the initial normalized acceleration. Eq. (14) agrees with Birdsall and Bridges,[4] [Section 5.04, Eq. (3)], up to the coefficients of the functions of θ. Substituting Eq. (14) into Eq. (5), integrating, and using the initial conditions leads to

$$X = X_O + Y_O' - FMq - A \sin(\theta + \beta) + (\overline{E}_O/2)\theta + (FMq/2)\theta^2 \tag{20}$$

$$X' = -A \cos(\theta + \beta) + \overline{E}_O/2 + FMq\theta \tag{21}$$

$$X'' = A \sin(\theta + \beta) + FMq . \tag{22}$$

From Eq. (3)

$$\Phi = \Phi_0 + 1 + 2M \sin \alpha^* + M^2 - X'^2 - Y'^2 . \tag{23}$$

With $M = 0$, this agrees with Birdsall and Bridges[4] [Section 5.05 Eq. (7)].

For $\alpha^* < \pi/2$, $X' > 0$ for all values of Y. For $\alpha^* > \pi/2$, $X' < 0$ for $Y - Y_0 < -\cos \alpha^*$ and $X' > 0$ for $Y - Y_0 > -\cos \alpha^*$. For $\alpha^* = \pi/2$, the trajectory is nearly straight for large q, wave shaped for $q_m < q \sim q_n$ (see Sections 3 and 4), U-shaped for reflected particles, and less than half a U if collected before reflection.

In summary, the trajectory of each particle is given by Eqs. (20) and (14) for $Y' \geqq 0$ and is symmetric for $Y' < 0$ (the particles turned back); the electric potential and field, before a turning point if any, are given by Eqs. (23) [with Eq. (21) and Eq. (15)] and Eq. (11) respectively; for case C, the electric field beyond the turning point equals the value at the turning point.

3. THE TURNING POINT

If the attracted particles can come to a point where $Y' = 0$, called "the turning point", generally the magnetic field reflects at least some of them back to the sheath edge. The limit of q for this occurrence and the value of θ, X, Y, and Φ at the turning point are now calculated.

From Eq. (15), case A (F = 1) occurs if and only if $A \leqq Mq$. From this and Eq. (17), the minimum value of q for case A is

$$q_m = \frac{a^2 + Y_0'^2}{2MY_0'} = \frac{\bar{E}_0^2/4 - \bar{E}_0 \cos \alpha^* + V_0^2}{2M(\sin \alpha^* + M)} . \tag{24}$$

q_m is a function only of initial (sheath edge) electric field (if any), entrance angle, and M.

For $q \leqq q_m$, from Eq. (15), τ, the value of θ which makes Y' first vanish, satisfies

$$\sin (\tau + \beta) = \frac{-FMq}{A} \tag{25}$$

$$\cos (\tau + \beta) = -\sqrt{1 - \frac{(FMq)^2}{A^2}} = \frac{-S}{A} , \tag{26}$$

8

where

$$S = \sqrt{A^2 - (FMq)^2} = \sqrt{a^2 + Y_o'(Y_o' - 2FMq)} \ . \tag{27}$$

The sign of the right-hand side of Eq. (26) is due to $\tau + \beta$ having to be in the third quadrant. Expanding $\sin \tau = \sin[(\tau + \beta) - \beta]$, $\cos \tau = \cos[(\tau + \beta) - \beta]$, and using Eqs. (18), (19), (25), and (26) leads to

$$\sin \tau = \frac{S(Y_o' - FMq) - aFMq}{A^2} \tag{28}$$

$$\cos \tau = -\frac{aS + FMq(Y_o' - FMq)}{A^2} \ . \tag{29}$$

By setting $\theta = \tau$ and substituting Eqs. (25) and (26) into Eqs. (20) and (14), we find the coordinates of the first stationary point for $q \leqq q_m$ to be

$$X_r = X_o + Y_o' + \frac{\overline{E}_o}{2} \tau + \frac{FMq}{2} \tau^2 \ , \tag{30}$$

$$Y_r = Y_o + a + S + FMq\tau \ . \tag{31}$$

This is usually the reflection point of the particle. The above results lead to the following deductions as q goes from a large to a small value.

<u>Case A:</u>
$q > q_m$: $S^2 < 0$, $F = 1$, $A < Mq$, the only case for which no stationary points exist.

$q = q_m$: the limit of case A, $S^2 = 0$, $F = 1$, $A = Mq$, $\sin \tau = -a/(Mq)$, and $\cos \tau = -(Y_o'/(Mq) - 1) = -\sqrt{1 - a^2/(Mq)^2}$. Stationary points also occur at $\theta = \tau + 2\pi i$, $i = 1, 2, 3, \ldots$ until the particles are collected.

<u>Case B:</u>
$q_m/2 < q < q_m$: $S^2 = 0$, $F = q_m/q$, $A = FMq$, and τ, X_r, Y_r, A, and the particle trajectories are independent of q. If the stationary point is before the object, it is a reflection point for $F-1$ fraction of the particles; the remaining $2-F$ fraction of the particles penetrate to the object.

Case C:

$q = q_m/2$: the limit of Case C, the maximum value of q for complete cutoff; all particles are reflected by the magnetic field unless the turning point is beyond the object surface. $S^2 = 0$, $F = 2$, $A = 2Mq$.

$q < q_m/2$: $S^2 > 0$, $F = 2$, $A > 2Mq$, and τ, X_r, and Y_r depend on q.

What are the limits of α, τ, q_m, and the reflection points as $Y_o \to 0$, what is the range of $\alpha*$, and what is the corresponding range of α?

For $M < 1$, the attracted species will enter the sheath,

$$0 < \alpha < \pi, \text{ for}$$

$$-\pi/2 < -\sin^{-1} M \leq \alpha* \leq \pi + \sin^{-1} M < 3\pi/2.$$

If also

$$-2\sqrt{1 - M^2} < \overline{E}_o < 2\sqrt{1 - M^2}, \text{ then for } 0 \leq \sin^{-1} M < \pi/2,$$

(1) as $\alpha* \to -\sin^{-1} M$:

$$a < 0, \ Y_o' \to \alpha \to \tau \to 0, q_m \to \infty, \ X_r \to X_o \text{ and } Y_r \to Y_o \text{ as they must, and}$$

(2) as $\alpha* \to \pi + \sin^{-1} M$:

$$a > 0, \ Y_o' \to 0, \ \alpha \to \pi, \ \pi \leq \tau \leq 2\pi, \ q_m \to \infty, \ X_r \to X_o + qM\tau^2,$$

$$\text{and } Y_r \to Y_o + 2\sqrt{1 - M^2} + 2qM\tau.$$

Physically, the magnetic field swings the particles away from the sheath in (1) and into the sheath in (2).

For $M > 1$:

$$0 < \cos^{-1} 1/M \leq \alpha \leq \pi - \cos^{-1} 1/M < \pi,$$

when

$$-\pi/2 + \cos^{-1} 1/M \geq \alpha* \geq -\pi/2 - \cos^{-1} 1/M \text{ and}$$

and when

$$-\pi/2 + \cos^{-1} 1/M \leq \alpha* \leq 3\pi/2 - \cos^{-1} 1/M.$$

For $E_o = 0$ (space charge limited),

$$q_m = \frac{V_o}{2M \sin \alpha} = \frac{1 - M^2}{2M (\sin \alpha^* + M)} + 1 \; . \tag{32}$$

This, for the three limits of M, is as follows.

(1) For $M \ll 1$, $q_m \cong 1/(2MY_o') + 1$. For a given value of M, the minimum value is $q_m = \frac{1}{2}\left[\frac{1}{M} + 1\right]$ for $\alpha^* = \alpha = \pi/2$. The maximum value is ∞ for $\alpha^* = -\sin^{-1} M$, $\alpha = 0$, or π.

(2) For $M \cong 1$ (strictly, for $|M - 1| \ll 1 + \sin \alpha^*$): $q_m \cong 1$. For $\sin \alpha^* \neq -1$ and $M = 1$, $q_m = 1$.

(3) For $M \gg 1$, $q_m \cong 1/2$.

From Eq. (32), three qualitatively different types of curves of $q_m(M)$ occur:

Type 1: $\sin \alpha^* = -1$, a singular case, $\vec{v}_g = -v_g \hat{y}$, shown as curve 1 of Figure 4. The thermal velocity is equal but opposite to the drift velocity, so $\dot{y}$ remains zero.

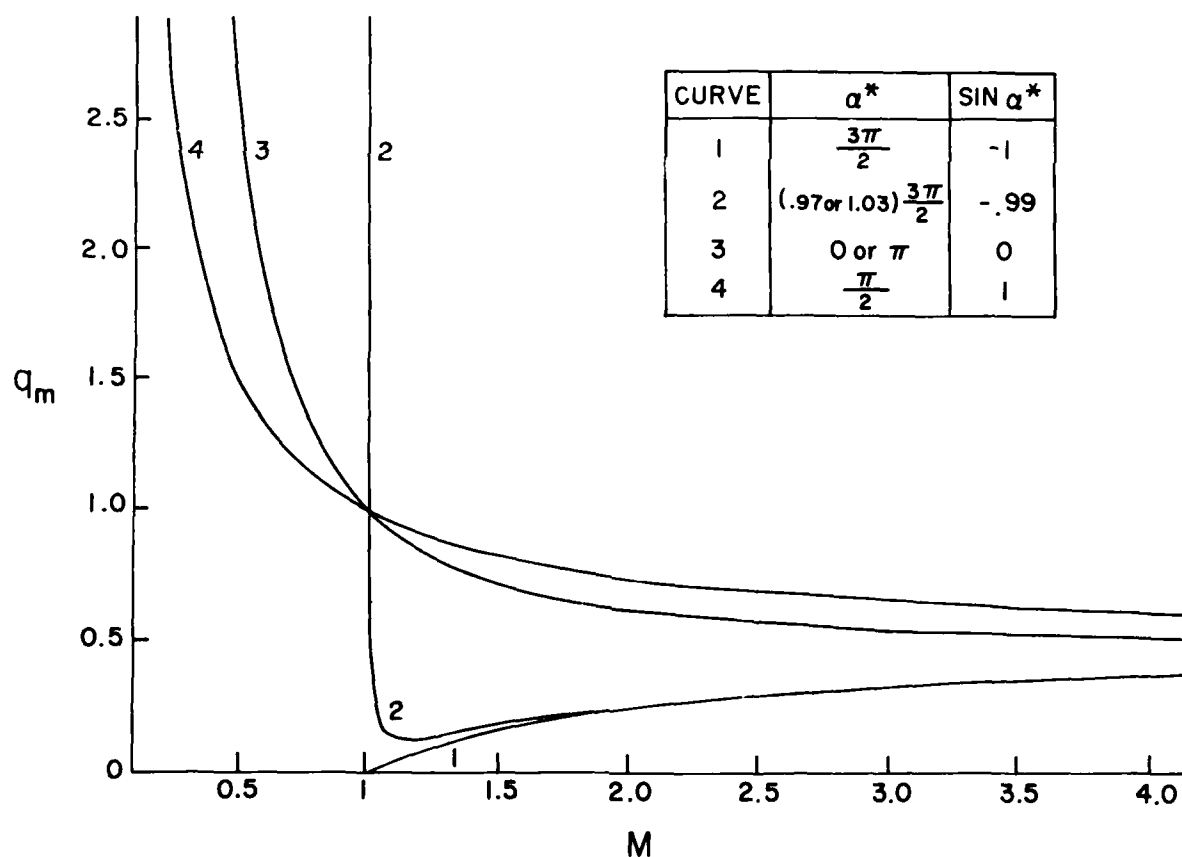| CURVE	α^*	SIN α^*
1	$\frac{3\pi}{2}$	-1
2	$(.97 \text{ or } 1.03)\frac{3\pi}{2}$	-.99
3	0 or π	0
4	$\frac{\pi}{2}$	1

Figure 4. q_m vs M for Some Values of α^*

11

Type 2: $-1 < \sin \alpha^* < 0$, $v_{gy} < 0$, between the limit of curve 2 as $\sin \alpha^* \to -1$ (the $M = 1$ line and curve 1) and curve 3 of Figure 4. In the plasma frame, the particle is moving away from the sheath; however, the sheath is moving faster, so it catches up to the particle. A minimum occurs at $M = M_m > 1$ and $q_m = q_{mm}$, where

$$\sin \alpha^* = - \frac{2M_m}{M_m^2 + 1} \tag{33}$$

$$q_{mm} = \frac{1}{2}[1 - \frac{1}{M_m^2}] . \tag{34}$$

A maximum occurs at $M = M_M < 1$, which also satisfies these two equations. But $q_m(M_M) < 0$; which is physically meaningless except that the sheath can never catch up to the particle.

Type 3: $\sin \alpha^* \geq 0$, $v_{gy} \geq 0$, between curves 3 and 4 of Figure 4.

What does this tell us about the effect of varying v_g from 0 ($M = \infty$) to the maximum value (minimum M = the larger of 0 and $-\sin \alpha^*$)?

(1) For type 1

    (a) $1 < q$: case A. (all incident particles collected)

    (b) $0.5 < q < 1$: case B (some particles collected) goes to case A.

    (c) $q < 0.5$: case C goes to case A. Case A exists up to $M = 1$.
    If $M < 1$, then $q_m < 0$, which is physically meaningless except
    that the particles can never cross the sheath edge.

(2) For type 2

    (a) $0.5 < q$: case A goes to case B at $M < M_m$, $q_m = q$, then
    finally to case C (no particles collected).

    (b) $0.25 < q < 0.5$: case B.

    (c) $q < 0.25$: case C may go to case B.

Either of the latter two may go to case A at $M_m < M$ and back to case B at $M < M_m$ before finally going to case C. For all of type 2, this final case C separates farther from case B without limit. That is, if $E_o = 0$, $0 < \sin^{-1} M < \pi/2$, and $-\sin \alpha^* < M \to -\sin \alpha^*$, then (i) $q_m \to \infty$, (ii) $X_r \to X_o$ and $Y_r \to Y_o$ for $-\sin^{-1} M \to \alpha^*$, and (iii) $X_r \to X_o + qM\tau^2$ and $Y_r \to Y_o + 2\sqrt{1 - M^2} + 2qM\tau$, $\pi < \tau < 2\pi$ for $\pi + \sin^{-1} M \to \alpha^*$. So, for sufficiently large $y_s - y_o$ (thus magnitude of object potential), finally the particles are reflected at $y = y_r$. If $M < -\sin \alpha^*$, then $q_m < 0$, which is physically meaningless except that the particles move away from the sheath edge, and so can never enter the sheath.

12

(3) For type 3

(a) $0.5 < q$: case A goes to case B, then finally to case C.

(b) $0.25 < q < 0.5$: case B goes finally to case C.

(c) $q < 0.25$: case C remains Case C. Case C separates farther from case B without limit: $q_m \to \infty$ as $M \to 0$. At first, this may contradict intuition since the effect of magnetic field must decrease. We see from Eq. (31), however, that y_r approaches a function that increases linearly with v_g as $M \to 0$; thus the particles penetrate the sheath without limit.

If $F = 1$, $E_o = 0$, and $q = q_m$, then

$$\tau = 2\alpha . \tag{35}$$

4. RANGE OF INCIDENT ANGLES

To get the range of incident angles, we consider the gyration phase angle before the particle enters the sheath at time $t = 0$, taken to be when the circle of gyration becomes tangent to the sheath edge. As before, a sharp sheath edge is assumed, and the plane surface and plasma are coming together along y with a relative velocity v_d. The coordinate system is chosen in the object frame with initial conditions as in Figure 5: the origin on the sheath edge and the gyrocenter a gyroradius, r_g, before it. The perpendicular component of velocity in the plasma frame is $v_g = \omega r_g$. In general, this β is different from the β used previously. The particle then is at
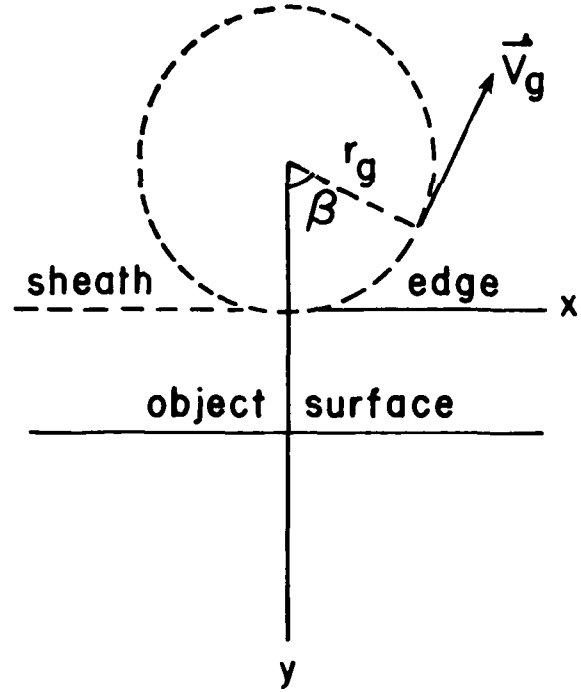
Figure 5. Coordinate System and Initial Conditions

$$x = r_g \sin(\omega t + \beta) \tag{36'}$$

$$y = v_d t - r_g [1 - \cos(\omega t + \beta)] . \tag{37'}$$

13

Normalizing as in Section 2,

$$X = \sin(\theta + \beta) \tag{36}$$

$$Y = M\theta - 1 + \cos(\theta + \beta) . \tag{37}$$

Let the subscript o designate the value for which $Y = 0$, and a prime designate the derivative with respect to θ. The entrance angle is determined from the values at the sheath edge of the derivatives of Eqs. (37) and (36):

$$\tan \alpha = \frac{Y'_o}{X'_o} = \frac{M - \sin(\theta_o + \beta)}{\cos(\theta_o + \beta)} . \tag{38}$$

Case 1. $M \leqq 1$.

Let β_1 be the value of β which makes θ_o the smallest non-negative value, θ_{o1}, for which $Y'_o = 0$, and let θ_{o2} be the next larger value of θ_o with $\beta = \beta_1$. The extrema of α occur for $\beta = \beta_1$: the minimum, 0, for $\theta = \theta_{o1}$, and the maximum for $\theta = \theta_{o2}$. Equating the numerator of Eq. (38) to zero,

$$\sin(\theta_{o1} + \beta_1) = M . \tag{39}$$

Using this in Eq. (37) = 0,

$$\theta_{o1} = (1/M)[1 - \cos(\theta_{o1} + \beta_1)] = M/[1 + \sqrt{1 - M^2}] . \tag{40}$$

From $\beta_1 = (\theta_{o1} + \beta_1) - \theta_{o1}$,

$$\beta_1 = \sin^{-1} M - M/[1 + \sqrt{1 - M^2}] . \tag{41}$$

A particle with a slightly larger value of β must gyrate through an additional angle $\theta_{o2} - \theta_{o1}$ (less than a gyration) before reaching the sheath edge, and then enters it at α_M, the largest value of α.

$$\theta_{o2} = (1/M)[1 - \cos(\theta_{o2} + \beta_1)] . \tag{42}$$

So, the range of α is

14

$$0 \leq \alpha \leq \alpha_M = \tan^{-1} \frac{M - \sin(\theta_{o2} + \beta_1)}{\cos(\theta_{o2} + \beta_1)} . \tag{43}$$

As $M \to 0$: $\theta_{o1} \to \beta_1 \to M/2$, $\theta_{o2} \to 2\pi - \alpha_M$, and $\alpha_M \to 2\sqrt{\pi M}$. At $M = 1$: $\theta_{o1} = \theta_{o2} = 1$, $\beta_1 = \pi/2 - 1$, and $\alpha_M = \pi$.

Case 2. $M \geq 1$.

Only one value of θ_o exists for each value of β. Solving Eq. (37) = 0 for $\cos(\theta_o + \beta)$ and substituting into Eq. (38),

$$\alpha = \tan^{-1} \frac{M - \sqrt{M\theta_o(2 - M\theta_o)}}{1 - M\theta_o}, \quad 0 \geq \theta_o \leq 2/M . \tag{44}$$

Differentiating this with respect to θ_o, equating to 0, solving for θ_o, and substituting into Eq. (44) leads to the minimum and maximum values:

$$\tan^{-1} \sqrt{M^2 - 1} \leq \alpha \leq \pi - \tan^{-1} \sqrt{M^2 - 1} . \tag{45}$$

As a numerical example, consider a satellite in a low earth orbit and assume that $T = 1000°K$, $v_d = 7$ km/sec, $n_\infty = 10^{11}$ m^{-3} and $B = 0.5 \times 10^{-4}$ T. Then, for electrons, $M_e = 0.05$, $0 \leq \alpha \leq 45°$, $14 < q_m < \infty$, and $q = 4.1$. For O$^+$ ions, $M_{O^+} = 8.4$, $83° \leq \alpha \geq 97°$, $0.44 < q_m < 0.56$, and $q = 1.2 \times 10^5$. So, the theory predicts that electrons with the mean thermal velocity would be reflected unless the distance from the sheath edge to the object surface were less than the reflection distance, that is, unless the magnitude of the object potential were small, whereas ions would be practically unaffected by the magnetic field. For attracted electrons with the numerical values above, Figure 6 shows normalized trajectories from the origin and Figure 7 normalized sheath potentials for three incident angles, all case C. The "trajectory" for $\alpha = 0$, curve 0 in Table 1, is the point at the origin.
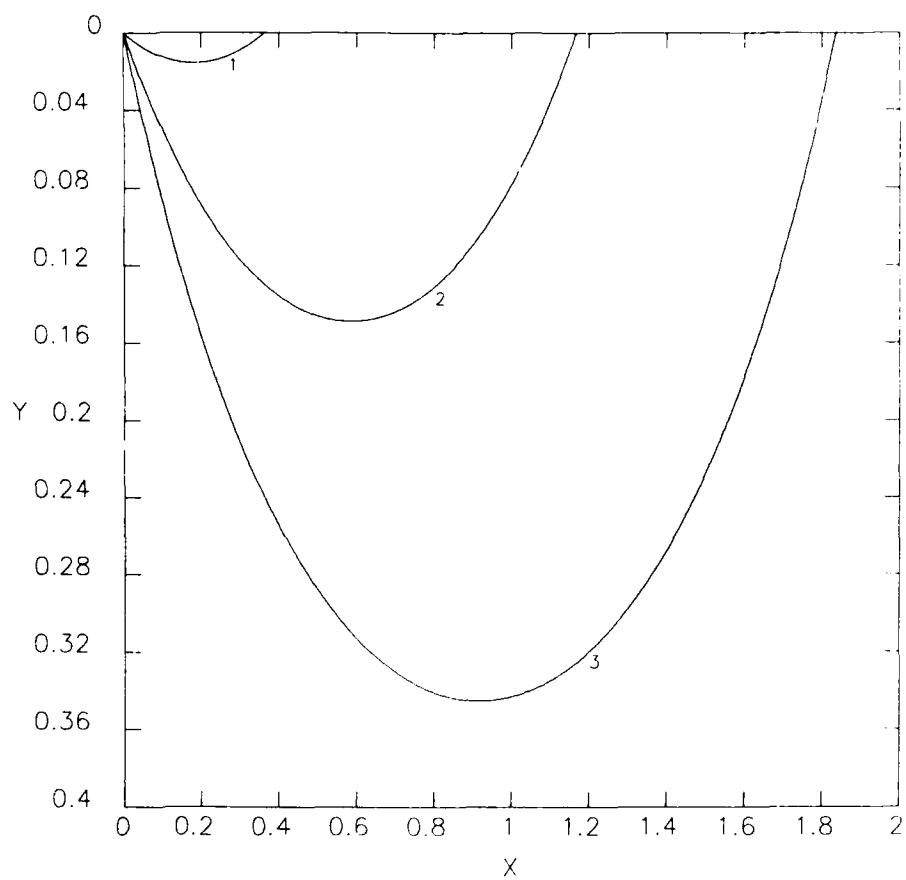
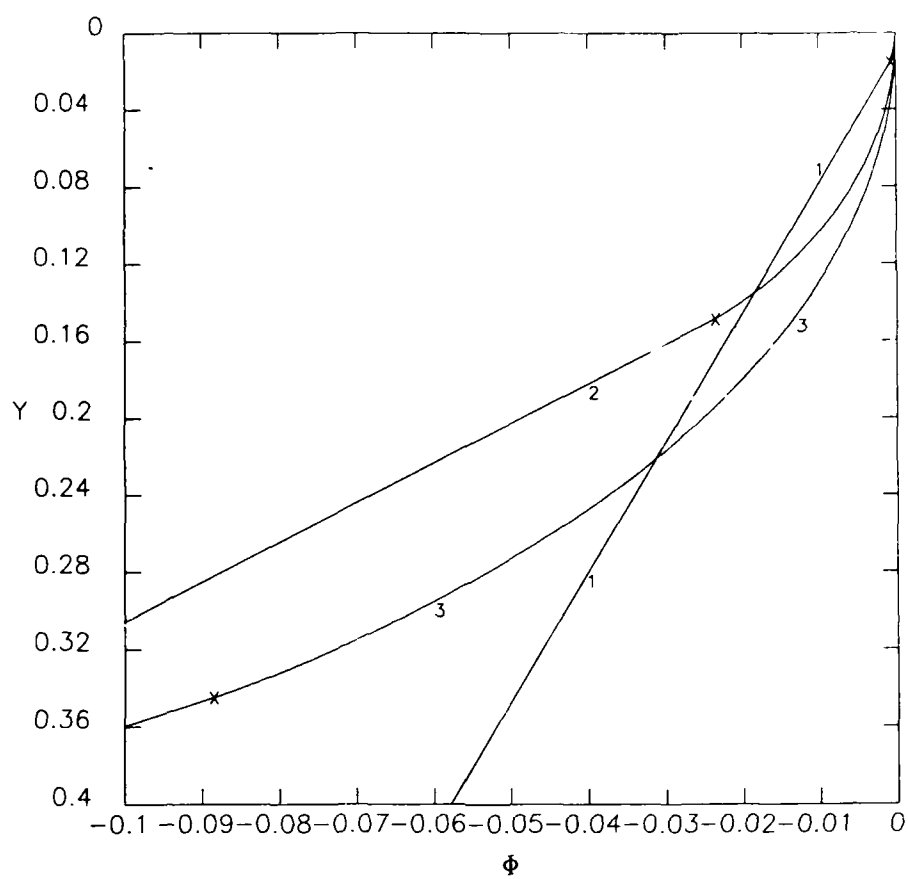Figure 6. Electron Trajectories. See Table 1

Figure 7.   Electron Sheath Potential.   See Table 1

Table 1. Parameters of Figures 6 and 7
$M = 0.05$, $q = 4.1$

Curve	α^*	α	q_m	β	τ	X_r	Y_r
0	-2.9°	0°	∞	202.3	0°	0	0
1	7.2	10	59.0	193.3	10.4	0.18	0.016
2	27.5	30	20.5	173.4	33.9	0.58	0.15
3	43.0	45	14.6	156.3	54.6	0.92	0.35

The x's in Figure 7 are at $Y = Y_r$. For $Y > Y_r$, the curves are linear since there is no charge and E is constant. Figures 8 and 9 are trajectories and potentials respectively for 0^+ ions, case A. The curves for the largest value of q are with the parameters in the first part of this paragraph, and are replotted in Figures 10, 11, and 12. With no magnetic field, Figure 10 and curve 2 of Figure 11 would be straight vertical lines. As expected, they show that the geomagnetic field deflects the ions very little. Also as expected, Figures 11 and 12 show a narrow range of incidence angles and potential distributions for 0^+ ions. Although this calculation is not realistic since the sheath edge is not really sharp and there is a distribution of velocities, it shows that, for low earth orbit conditions, the predominant values of α are low for electrons (object positively charged) and near 90° for ions (object negatively charged). Also, as expected, generally ions are affected very little whereas electrons are greatly affected by the magnetic field.
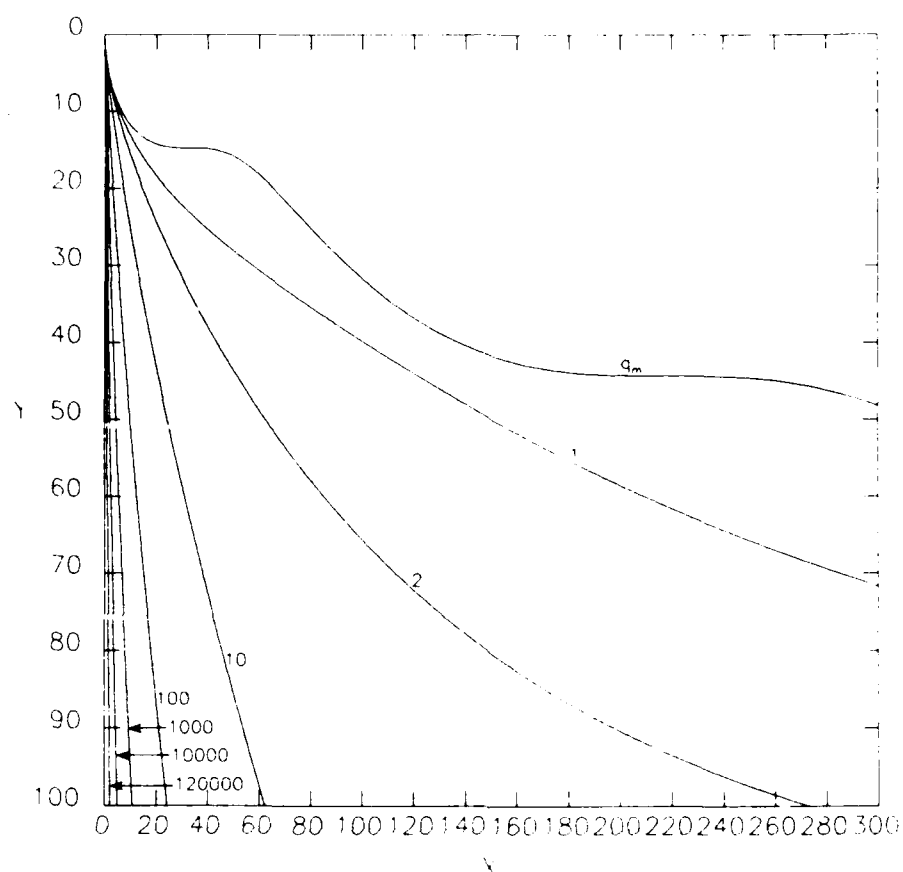
18

Figure 8. 0^+ Trajectories for Various Values of q.
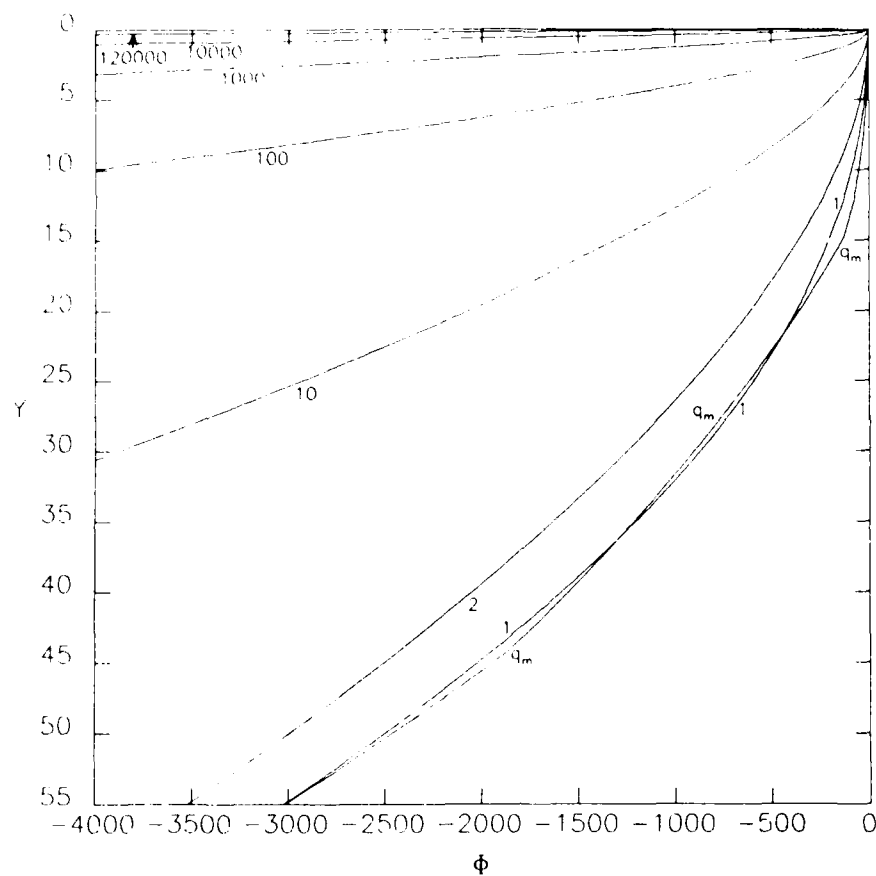$M = 3.4$, $q_m = 0.5595$, $\alpha^* = \alpha = 90°$

Figure 9. 0^+ Sheath Potential for Various Values of q.
M = 8.4, q_m = 0.5595, $\alpha^* = \alpha = 90°$

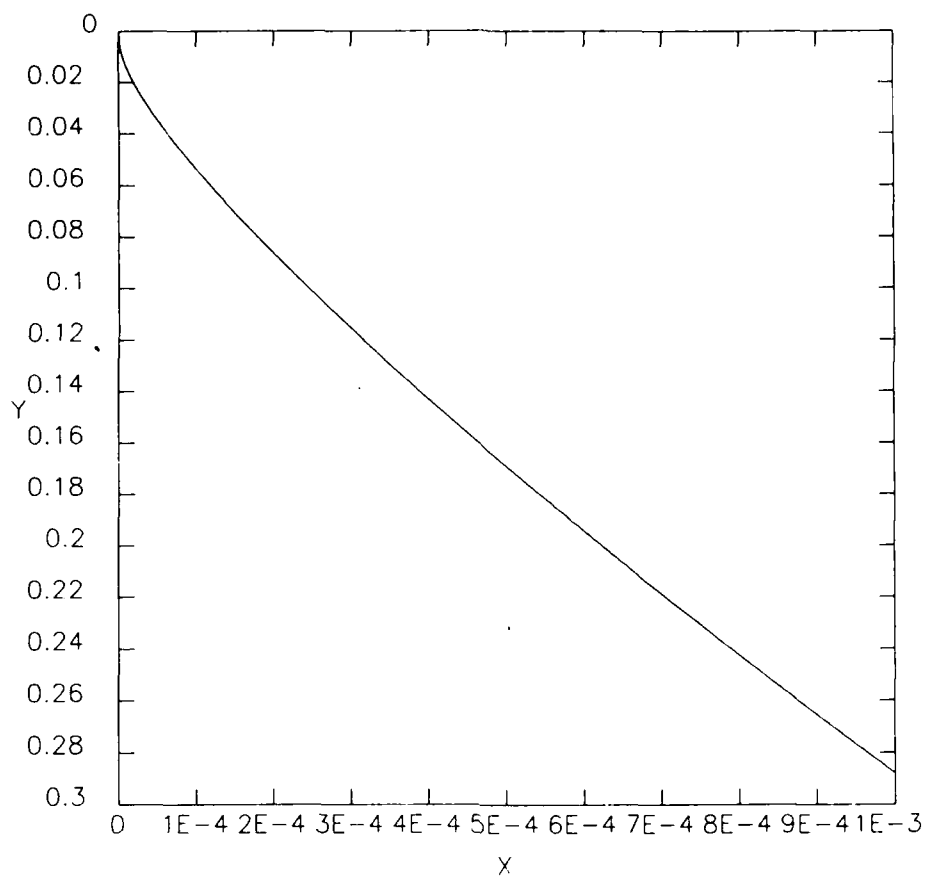Figure 10. 0^+ Trajectory. $M = 8.1$, $q = 120,000$, $q_m = 0.5595$, $\alpha^* = \alpha = 90°$

Figure 11.   Range of 0^+ Trajectories.   M = 8.4, q = 120,000,
$\beta = \pi/2$.   1: minimum α^* & α. q_m = 0.5, $\alpha^* = $ -6.84°,
α - 83.16°, 2: q_m = 0.5595, $\alpha^* = \alpha$ - 90°, 3: maximum α^* & α.
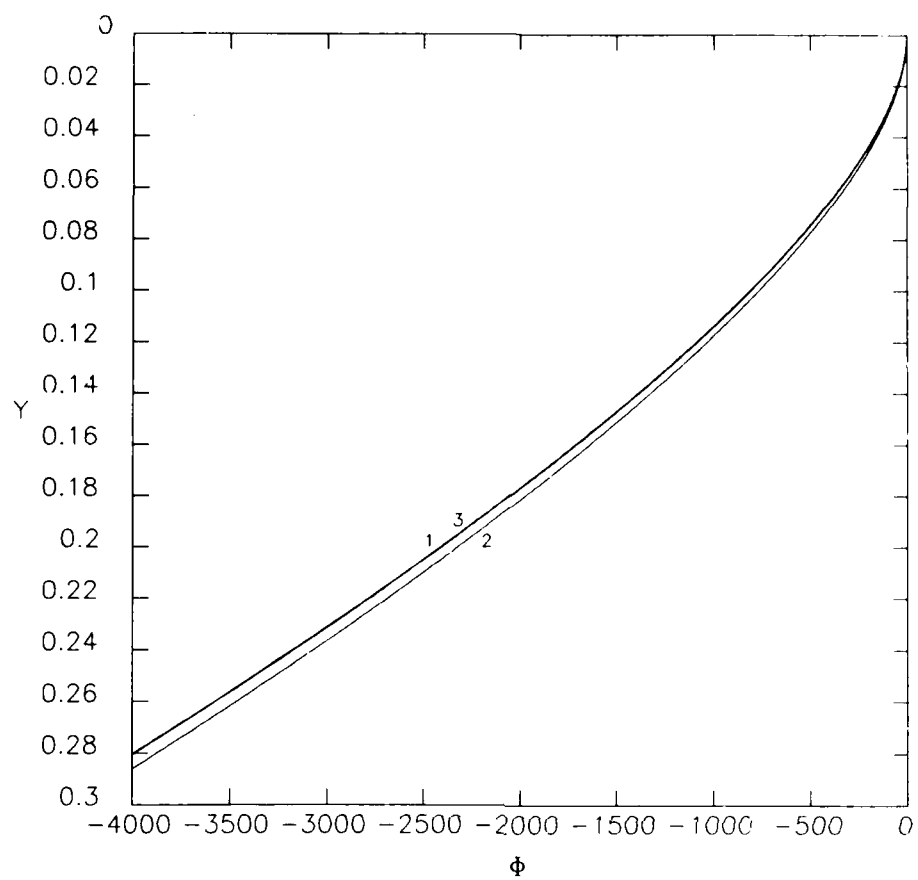q_m = 0.5, α^* - 136.84°, α = 96.84°

22

Figure 12. Range of Sheath Potentials. Same parameters as in Figure 11

5. STABILITY OF A CUTOFF SHEATH

Section 3 shows that, for this simplified case and $q < q_m/2$, all of the attracted particles are reflected away from the object plane at a certain $y = y_r$ (if $y_s > y_r$, see Figure 13), making a vacuum insulation gap. The theory also shows that the difference in object and reflection point potentials, $\phi_s - \phi_r$, is proportional to $y_s - y_r$; thus the gap increases with increasing $|\phi_s|$. This is consistent with the repelled species being repelled farther from the object for ϕ_s larger. Is this result of the theory correct? Here, we consider this question. First, we assume a gap and determine whether or not it tends to close (decrease in thickness). Let σ_s be the surface charge density on the object and σ_c be the sheath charge in a column of unit cross section area from y_o to y.
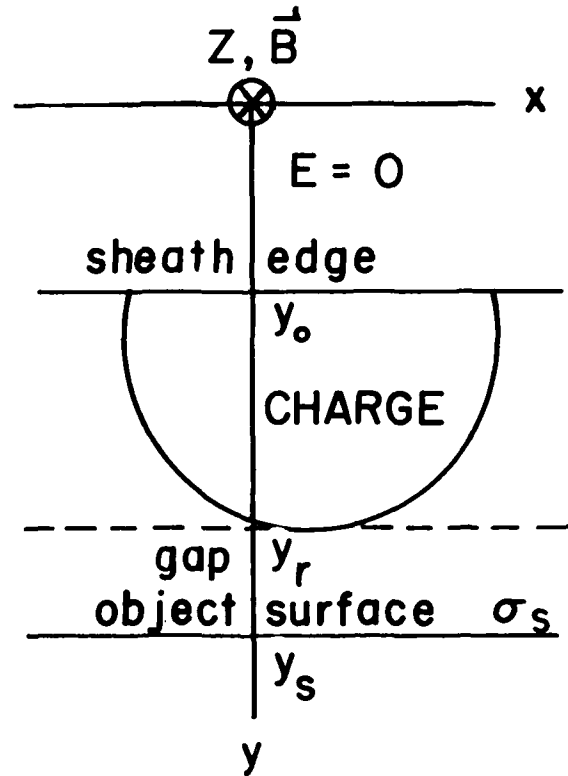

Figure 13.   Insulation Gap

$$\sigma_c = \int_{y_o}^{y} sn e \, dy = se \int_{0}^{\theta} \frac{FMn_\infty}{Y'} \dot{y} \, dt = sFn_\infty \, ev_d \, \theta / \omega, \qquad (46)$$

from Eq. (9) and the normalization in Section 2. For $y_r \leq y < y_s$:

$$\sigma_c = \sigma_{cM} \equiv sFn_\infty \, ev_d \, \tau / \omega , \qquad (47)$$

the total charge per unit area in the sheath. So, in general, $\sigma_c \leq \sigma_{cM}$, and $\Phi_s \to \Phi_o$ as $Y_o \to Y_s$. We start with $\sigma_s = -\sigma_{cM}$ ($E_o = 0$) and the object isolated. A variation of Y_o, δY_o, with Y_s fixed causes no variation in σ_{cM} while $y_s > y_r$ and no variation in σ_s since the current to the object is zero (although the object potential varies). (The same results would be obtained by varying y_s instead of y_o.) Therefore, $\delta E_o = 0$ so that $\delta a = \delta A = \delta S = 0$. Also, from Eq (47), $\delta \tau = 0$. The maximum magnitude of magnetic field due to the current is at $y = y_o$ or y_r and may

24

be shown to be $\mu_0 I/2$, $I = \int_{y_0}^{y_r} j_x dy$, $j_x = ne\dot{x}$. From Eqs. (9), (21), and the normalization, then applying the result to the case in Table 1 giving the largest field, that is, curve 3, we obtain $2 \times 10^{-6} B$. Thus, the magnetic energy is quite accurately only that due to the ambient magnetic field, so, effectively, it does not vary with y_0 or anything else. The electrical energy is that in the charge, W_c, plus that in the insulation gap, W_g. Letting a line over a quantity designate its normalized value:

$$\overline{W} = \overline{W}_c + \overline{W}_g, \quad 2\overline{W}_c \equiv \int_{Y_0}^{Y_r} \overline{E}_c^2 \, dY, \quad 2\overline{W}_g \equiv \int_{Y_r}^{Y_s} \overline{E}_g^2 \, dY .$$

$F = 2$, so,

$$\overline{E}_c = \overline{E}_0 + 4Mq\theta, \quad Y_0 \leqq Y \leqq Y_r \tag{48}$$

$$\overline{E}_g = s \frac{2e\sigma_s}{\epsilon_0 m \omega v_g}, \quad Y_r \leqq Y \leqq Y_s \tag{49}$$

$$2\overline{W}_c = \int_0^\tau \overline{E}_c^2 Y' \, d\theta . \tag{50}$$

From Eqs. (15), (44), and (46), W_c is seen not to vary with Y_0. From Eq. (31), we note that the sheath charge thickness, $Y_r - Y_0$, does not vary with Y_0. $\overline{E}_g$ does not vary with Y_0, so

$$\delta 2\overline{W} = \overline{E}_g^2 \delta(Y_s - Y_r) = - \overline{E}_g^2 \delta Y_0 \tag{51}$$

from Eq. (31) since Y_s is fixed. Since charges tend to move to minimize the electrical energy, in accord with the plates of a condenser tending to collapse, Y_0 tends to increase. Nevertheless, the theory here indicates that, because of the magnetic as well as the electric field, the particles gyrate and drift along the x axis so that, for $q < q_m/2$ and $|\Phi_s|$ large enough to make $Y_r < Y_s$: an insulation gap, $Y_s - Y_r$, is maintained. However, the theory assumes that the reflected attracted and repelled particles disappear after exiting or bouncing off the sheath edge. Assuming a plane, sharp sheath edge, calculating two ion reflections and three electron gyrations for the case of curve 3, Section 4 leads to the following inductions. Both species gyrate (in opposite senses), reenter the sheath, reexit, reenter, and so on. After first reaching the sheath edge, due to the motion between plasma

and object, they gain energy and penetrate more each gyration, approaching remaining in the sheath, that is, with their minimum value of y being $y = 0$. This makes the effective sheath edge closer to the object by the penetration depth of the repelled species. This contradicts the theory here. Simultaneously, both species drift (in the +x direction for $\vec{B} = -\hat{z}B$). More importantly, the number density of each species near the sheath edge increases by the ambient number density each gyration. So the electron number density increases much faster than that of the ion. If the object is positively charged, the effective q increases just as rapidly since $q \propto n$ according to the theory. For example, for curve 3 in Section 4, the effective electron q would be greater than η_m after four gyrations, about 4 μs. Furthermore, α increases each gyration, so, if $\alpha \lesssim 83°$, as it is for the first four gyrations of the numerical electron cases of Section 4, q_m decreases. So, case C goes rapidly to case A or B with no insulation gap. The conduction current will drain off the excess electrons so that, either case C (or B) is produced and conduction and (partial) insulation alternately occur, or case B is maintained. Taking a distribution of particle velocities into account, some of the higher energy particles with $\sin \alpha^* > 0$ (type 3, see Section 3) will penetrate to the object. These considerations and perhaps others thus show that a vacuum insulation gap is not expected to exist, although a region of low density may. We speculate that essentially these phenomena would occur over most of a positively charged plate with sufficiently large size and potential.

If the object potential and y_s are held constant while y_o is increased (the gap decreased), the amount of charge in the sheath would have to increase (unless E_o changes) since the capacitance per unit area increases. But Eqs. (28), (29), and (47) are independent of y_o, so this contradicts the theory.

6. CONCLUSIONS

An infinitely large, uniformly charged plane moving perpendicular to its surface in a magnetoplasma is considered. Analytic, self consistent equations of electric field in the sheath and trajectories of the attracted species through the sheath are obtained. A uniform magnetic field parallel to the plane surface, negligible collisions, one velocity of only the attracted species moving into the sheath, and a sharp sheath edge are assumed. Uniformity of magnetic field and negligible collisions are generally accurate assumptions for an object in low earth orbit or higher. Collisions are expected to have an appreciable effect if the object size is comparable to a collision mean free path. The assumptions of a single velocity and a sharp sheath edge are inaccurate. Nevertheless, the physical trends of most of the results obtained here should be correct. Even though the object

26

moves relative to the plasma, the solution is basically the same as that obtained much earlier for a planar magnetron.

The effect of a magnetic field is determined by the value of q which is a constant times n_∞ / B^2. If it is much larger than the cutoff q, then the magnetic field has little effect. The cutoff q, q_m, is a function only of sheath entrance angle and M. For M << 1, it goes from near $1/(2M)$ at vertical incidence to ∞ at grazing incidence in the object frame. It equals 1 for M = 1 and 1/2 for M >> 1. Thus q_m, and therefore the effect of a magnetic field can be quite large at all values of q for sufficiently small values of M. This is expected, since the effect of a magnetic field increases with decreasing particle energy. For $q < q_m$ and the magnitude of the object potential small enough for the reflection distance, $y_r - y_o$, to be large compared to the sheath thickness, $y_s - y_o$, the magnetic field has little effect.

Numerical examples are calculated for typical low earth orbit conditions. For attracted electrons, the range of incidence angles is found to be below $45°$, $M \simeq 0.05$, and $q \simeq 4$. The latter is less than q_m which is greater than 14. For attracted 0^+ ions, the incident angle is within $7°$ of the vertical, $M \simeq 8$, $q \simeq 10^5$, much larger than q_m which is 0.5. So the magnetic field affects electrons greatly, but it affects ions negligibly.

The solution presented here for this simple case, including the reflection distance, depends only on M, sheath entrance angle, and q. It shows that, as the magnitude of the object potential increases, the trajectories and potential function do not change; the sheath just thickens, or, if there is an insulation gap, the gap increases. However, other effects (next paragraph) change this picture.

A stability analysis led to the conclusion that an insulation gap between the charged sheath and the object would tend to narrow and thus to vanish. With a sufficient magnetic field and magnitude of potential, however, the theory indicates that the magnetic field swings the attracted particles clear of the object so that a gap would exist. But the theory assumes that after the repelled species hit the sheath edge and after the attracted species exit the sheath, the particles disappear. Actually, the magnetic field causes any exiting particles to reenter. Assumption of a plane, sharp sheath edge and calculation of a few gyrations through the sheath edge results in the particles increasing in number, energy, and penetration each gyration, and to the speculation that the state either oscillates between cases (B or C) and A or remains case B. Also, the high energy tail of a realistic velocity distribution would penetrate to the plane. So, a perfect insulation gap could never exist, although a low density region may exist part of the time near the object. We speculate that basically these phenomena would occur over most of a positively charged, finite plane as considered here, if its size and potential are sufficiently large. Penetration of the sheath edge by the repelled species results in a

contradiction to the theory. Unless the object plane is large compared to the attracted species gyroradius, edge effects would also be important. So, clearly a much better, perhaps two or three dimensional treatment, is needed, one with a more realistic sheath edge that integrates over all angles of sheath entry and the speed distribution. Since such a treatment cannot be done analytically, it must be done numerically. Such a theory would resolve the specific questions raised above.

References

1. Page, L., and Adams, N. I. (1946) Space charge in cylindrical magnetron, Phys. Rev., 69:494-500.

2. Page, L., and Adams, N. I. (1958) Principles of Electricity, 3rd Ed., D. Van Nostrand.

3. Benham, W. E. (1935) Electronic theory and the magnetron oscillator Proc. Phys. Soc., (London) 47:1-53.

4. Birdsall, C. K., and Bridges, W. B. (1966) Electron Dynamics of Diode Regions, Academic Press, Chapter 5.

5. Linson, R. H. (1969) Current-voltage characteristics of an electron-emitting satellite in the ionosphere, J. Geophys. Res., 74:2368-2375.